

## CHAPTER 5

### ELECTROPHORESIS OF AgI SOLS IN AQUEOUS SOLUTIONS (EFFECT OF IODIDE ION AND ANIONIC AND CATIONIC SURFACE ACTIVE AGENTS)

#### 5.1. Introduction :

In the last two chapters we have described the results of electrophoretic mobility measurements using droplets of two organic liquids, in distilled water and electrolyte solutions. Since the results obtained have been analysed in terms of the W.L.O. theory which is valid strictly for solid particles only, therefore, it was deemed desirable to secure mobility results using solid particles. For this purpose AgI sols were considered to be the most satisfactory, because (i) stable sols in the size range suitable for microscopic observation can easily be prepared, (ii) the properties of the double layer of AgI sol particles have been extensively investigated earlier,<sup>55)</sup> and (iii) results of recent accurate mobility measurements with application of relaxation correction theories<sup>88,89)</sup> are available in the literature, for purpose of comparison.

For the above reasons AgI sol was chosen for our investigations, which centred mainly on the study of the applicability of the W.L.O. theory to the results so obtained. As explained earlier, results of mobility measurements for particles of varying sizes in constant electrolyte concentration solutions are required for this purpose. Unfortunately, it was found that particles of significantly different sizes could not be conveniently studied, because the rate of settling under gravity in the microelectrophoresis cell increased rapidly with increasing particle size.

A different aspect of the property of the double layer of AgI sol particles was therefore chosen for investigation. This was the effect of large sized (surface active) counter-ions and co-ions on the  $\zeta$  potential of AgI sol. In the present chapter the results of these studies are discussed.

#### 5.2. Study of AgI sols in presence of surface active agents :

Many organic ions are known to produce coagulation of hydrophobic sols at very

low ionic concentrations; this has been termed "sensitised coagulation"<sup>55)</sup>. In general, such ions reverse the charge of the sol, and eventually a stable sol of opposite charge is produced<sup>90)</sup>. Although, the influence on sol stability of a number of large ions including strychnine<sup>91,92)</sup>, morphine<sup>92)</sup>, guanidine<sup>92)</sup>, dodecyl-pyridinium<sup>90,93)</sup>, dodecyl sulphate<sup>93,94,95)</sup> and dodecyl amine<sup>95)</sup> has been studied, most of this work has been purely qualitative.

Lately, Ottewill and coworkers<sup>88,89)</sup> have adapted the Derjaguin-Verwey-Overbeek<sup>10,96)</sup> theory of colloid stability for the case of adsorption of ions of surface active agents on the surface of colloid particles, and have co-related the stability with the concentration of such ions in solution. These workers have used AgI sols of small particle size, at a constant concentration of the potential-determining ions in solutions ( $pI^-$  constant), which is large enough compared with the (varying) concentration of the surface active ions added (so as to render  $\kappa$  almost constant), and yet small enough so that  $\kappa a$  remains small and the Debye-Hückel approximation remains valid.

As the surface potential is known to be critically dependent on the concentration of the potential determining ions in solution therefore it becomes of some interest to study the effect of surface active ions on the properties of a sol, at different concentrations of the potential determining ions in solution. However, the simplifying condition of  $\kappa$  constant may be lost thereby and the detailed correlation of stability with the concentration of surface active ions may no longer be as simple as in the Ottewill treatment.

We have therefore studied the dependence of the electrokinetic behaviour of AgI sol particles on the concentration of surface active ions, at different constant concentrations of potential determining ions. By the addition of KI or  $AgNO_3$  the iodide ion concentration could be varied over a large range ( $10^{-2}N$  to  $10^{-13}N$ ), and the entire course of variation of  $\zeta$  with  $I^-$  ion concentration, including charge reversal, was first established; sols containing different concentration of  $I^-$  ions (four on the

negative charge side, and three on the positive charge side), were then used for the study of the effect of concentration of suitable surface active counter-ions (cetyl trimethyl ammonium, cetyl pyridinium and dodecyl sulphate). The mobility values obtained were then used for the calculation of the  $\zeta$  potential values, using for this purpose the W.L.O. method, as before.

5.3. Materials used and preparation of the AgI sols :

(i) Chemicals used :

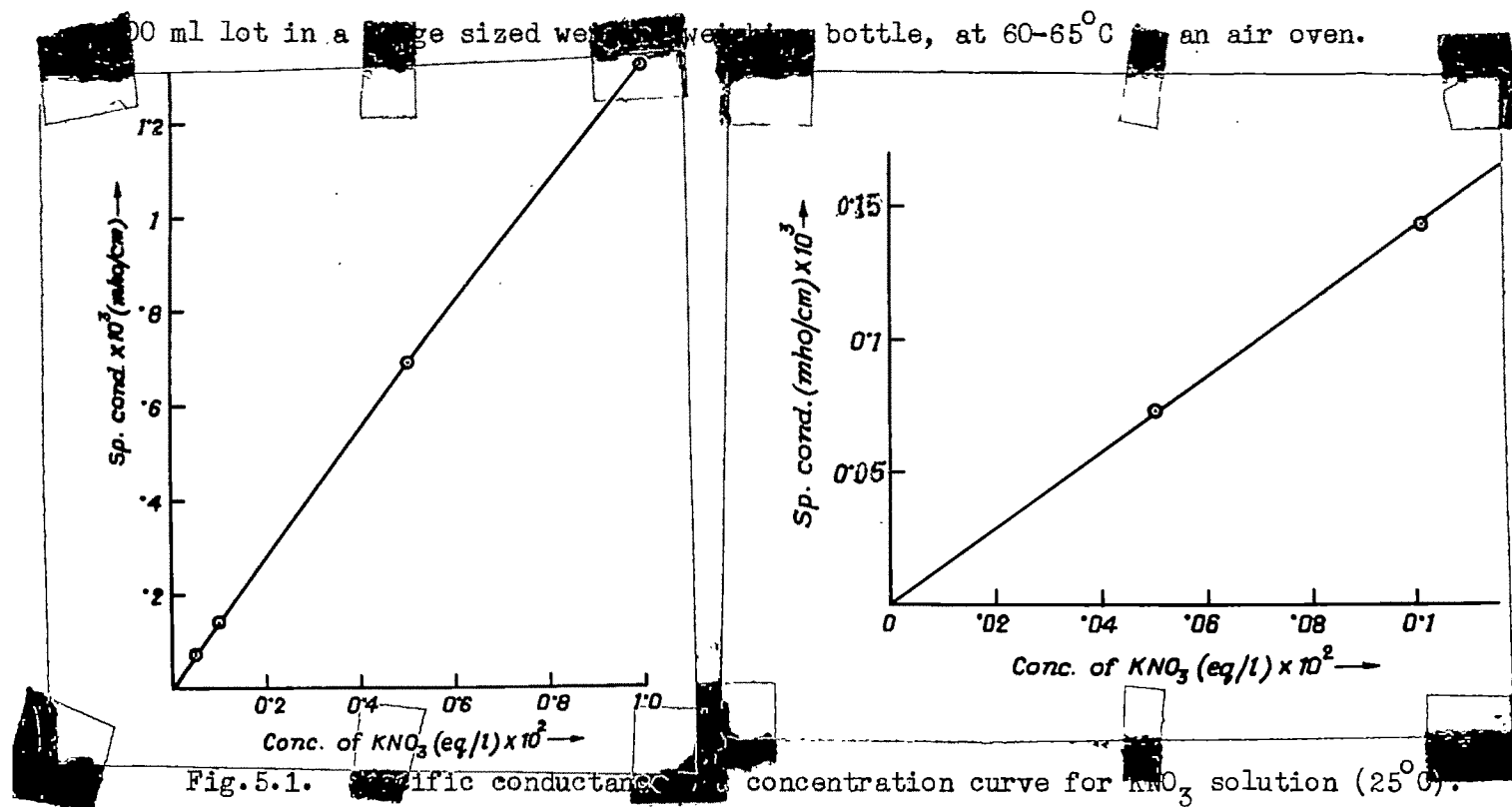
- a. The silver nitrate and potassium iodide used were A.R. grade.
- b. Cetyl trimethyl ammonium bromide (CTAB) was from Eastman Kodak Company.
- c. Cetyl pyridinium chloride (CPyCl) was of L. Light Co.
- d. Sodium dodecyl sulphate (NaDS) was of purity 97.5%.

(ii) The AgI sol was prepared<sup>83)</sup> by adding equal volumes of 1.25 mM  $\text{AgNO}_3$  solution slowly to 1.38 mM KI solution with vigorous stirring by means of a mechanical stirrer. The sol so prepared was aged at  $70 \pm 2^\circ\text{C}$ . for 12 hours, dialysed in cellophane bags to a minimum possible concentration of electrolytes, and then passed twice through successive columns of strong acid and strong base ion exchange resin (Amberlite IR-120 and IRA-400). Two lots of sols were prepared. The sol thus prepared (sp. cond.  $1.06 \times 10^{-6}$  mho/cm for the first lot and  $1.728 \times 10^{-6}$  mho/cm for the second lot) was unstable because of the almost complete removal of the ions originally present (such as  $\text{KNO}_3$  produced, and some excess KI, in the molar ratio  $\sim 9:1$ , as calculated). The total residual concentration of the electrolyte (assumed to be  $\text{KNO}_3$ ) was estimated for both lots from their specific conductivity, by use of a sp. cond. vs. concentration plot for  $\text{KNO}_3$  (Fig. 5.1) as prepared from literature data<sup>73,97)</sup> in the very low  $\text{KNO}_3$  concentration region ( $25^\circ\text{C}$ ). These concentrations were thus estimated to be  $5.0 \times 10^{-6}$  N for the 1st lot and  $5.52 \times 10^{-6}$  N for the 2nd lot.

In order to obtain reasonably stable sols, without increasing the electrolyte concentration unnecessarily, the minimum required concentration in the sol of the stabilising electrolyte KI was first ascertained by trial, and was found to be  $3 \times 10^{-5}$  N.

This KI concentration in both lots of the sol was secured by adding (immediately after the ion-exchange resin treatment) suitable amount of KI.

The sols thus prepared were very dilute, for convenience in microscopic mobility measurements. The colloid content of the AgI sol was determined by evaporation of a



#### 5.4. Experimental procedure :

The general details of experimental procedure were similar to that described in the case of the oil emulsion (Chapter 3). Some other salient details were as follows:

- (i) For work with surface active agents, all pipettes etc. used were thoroughly rinsed with the experimental solution before carrying out dilutions, etc. The microelectrophoresis cell was also rinsed and kept filled for about 2 hours prior to experiment with a surfactant solution of concentration equal to that of the experimental solution, in order to saturate the glass surface before the final filling.
- (ii) Different lots of the sol having different  $\text{I}^-$  concentrations were prepared by the addition of requisite amounts of KI or  $\text{AgNO}_3$  to the stock sol. The  $\text{I}^-$  concentration of the different lots were measured potentiometrically.

Ag-AgI electrode was prepared by depositing metallic silver on platinum coil by thermal decomposition of scrupulously purified  $\text{Ag}_2\text{O}$  and then depositing  $\text{I}^-$  ion on silver by electrolysis from acidified pure KI solution ( $\sim 0.1\text{N}$ )<sup>86</sup>. The electrode so prepared was characterised by measuring the  $E_{\text{Ag-AgI}}^0$ . This was determined from potential measurements in HI solutions of different known concentrations (by titration), in conjunction with a (platinised platinum) hydrogen-electrode, and proper extrapolation (Fig.5.3). Two electrodes were prepared :

(a) The electrode having  $E_{\text{Ag-AgI}}^0 = 0.1452$  volt was used for measuring the  $\text{I}^-$  ion concentration in systems where no surface active ions were present (the effect of  $\text{I}^-$  ion concentration only on electrophoretic mobility being studied) by coupling with a saturated calomel half-cell. The  $\text{I}^-$  concentration of the original stock sol ( $3.36 \times 10^{-5}\text{N}$ ) could be reliably determined by titrating potentiometrically with standard (very dilute)  $\text{AgNO}_3$  solution (Fig.5.2). The  $\text{I}^-$  concentrations of the other

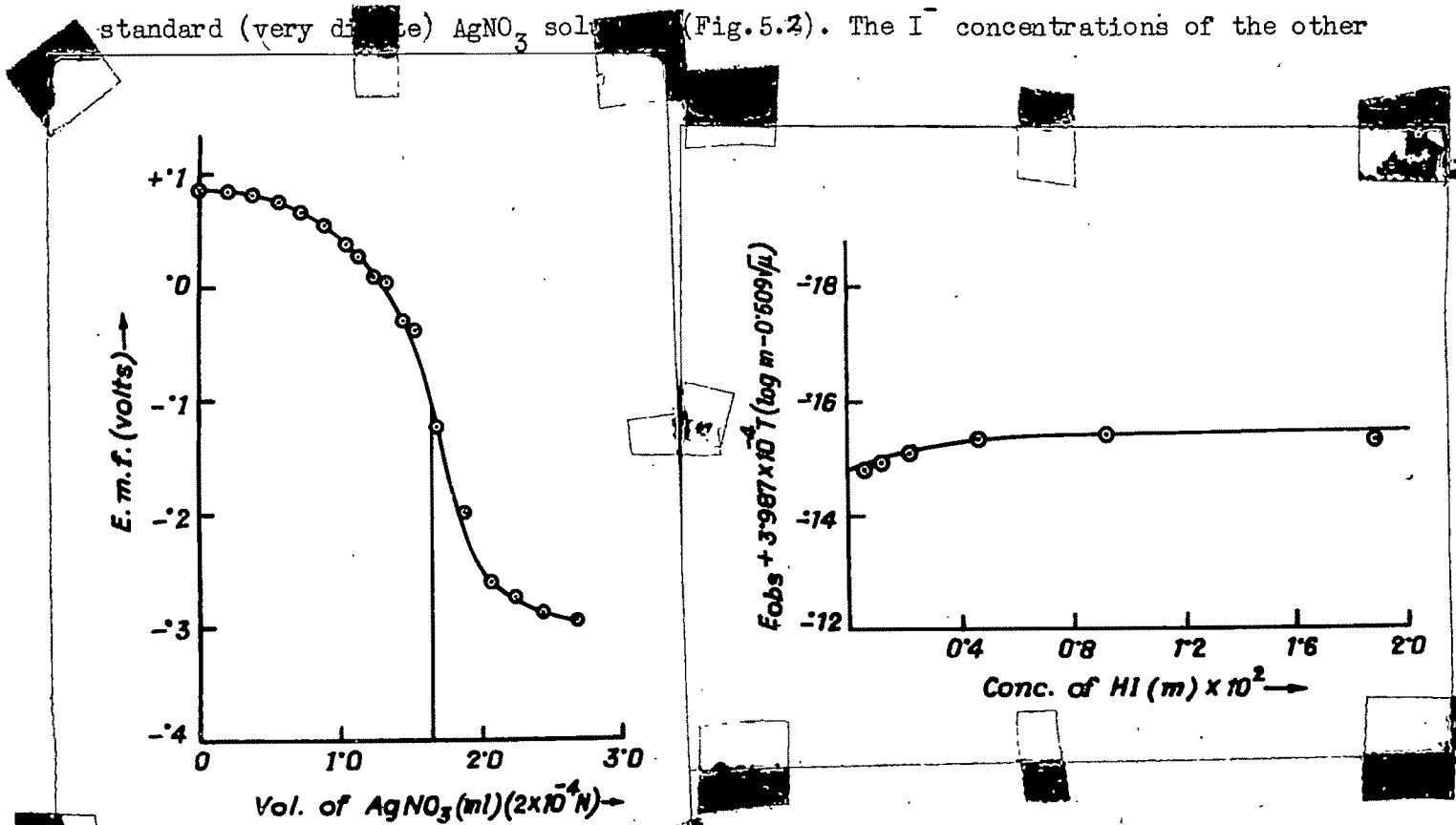


Fig.5.2. Potentiometric titration of  $\text{I}^-$  in the stock sol with dilute  $\text{AgNO}_3$  solution.

Fig.5.3. Determination of  $E_{\text{Ag-AgI}}^0$  (Harned and Owen; ref. 97, p.459).

sols were calculated from the measured cell c.m.f.s ( $E_{\text{sol}}$ ) by using the equation

$$\Delta E = E_{(\text{stock sol})} - E_{(\text{sol})} = RT \ln \frac{3.36 \times 10^{-5}}{a_{\text{I}^-}} \quad \dots(5.1)$$

$E_{(\text{stock sol})} = 0.0854$  volt being the cell e.m.f. using the stock sol.

(b) For the determination of  $\text{I}^-$  ion concentration in mixtures of the sol with surface active ions the electrode having  $E_{\text{Ag-AgI}}^{\circ} = 0.1440$  volt was used in conjunction with a Ag-AgCl electrode (of known  $E^{\circ} = 0.2215$  volt) in known  $\text{Cl}^-$  ion ( $1.128 \times 10^{-2} \text{N}$ ) concentration (via a saturated  $\text{KNO}_3$  bridge). The equation used was :

$$E_{\text{obs}} = E_{\text{Ag-AgCl}}^{\circ} + E_{\text{Ag-AgI}}^{\circ} + 0.0591 \log \frac{a_{\text{I}^-}}{a_{\text{Cl}^-}} \quad \dots(5.2)$$

(iii) Electrophoresis measurements were carried out in the conventional electrophoresis cell, at room temperature.

(a) The variation of electrophoretic mobility (and hence  $\zeta$  potential) with  $\text{I}^-$  concentration was first studied (using the first lot of the sol prepared). The range of variation of  $\text{I}^-$  concentration was from  $\sim 10^{-2} \text{N}$  to  $\sim 10^{-13} \text{N}$ . This variation was attained as described earlier. The  $\text{I}^-$  concentrations of different lots thus prepared were determined potentiometrically as discussed above, and are recorded (at the top) in the Table (5.1).

In the case when  $\text{AgNO}_3$  was added to the stock sol (containing  $3.36 \times 10^{-5} \text{N I}^-$ ),  $\text{KNO}_3$  was produced, so that its concentration in such lots of the sol was larger than that in the stock sol; these  $\text{KNO}_3$  concentrations are recorded in Table (5.1) (After the first or second addition of  $\text{AgNO}_3$ , the  $\text{KNO}_3$  produced on further addition was very small, so that its concentration remained almost unchanged thereafter). The  $\text{I}^-$  concentrations were simultaneously decreased, and the values (determined potentiometrically) are also given in Table (5.1). The solubility product of AgI being  $8.5 \times 10^{-17}$ <sup>85</sup>, when the  $\text{I}^-$  concentration was reduced to below the value  $\sim 9.0 \times 10^{-9}$ , on further addition of  $\text{AgNO}_3$  to the stock sol the  $\text{Ag}^+$  concentration (calculated) in

the sol produced was larger than the  $I^-$  concentration, and is also recorded in Table 5.1.

The results of electrophoretic mobility measurements, with variation of  $I^-$  concentration only, are recorded in Table 5.1. The  $\zeta$  potentials were calculated by the W.L.O. method after introducing particle-size correction and ionic mobility correction (details given later, p.118). The variation of  $\zeta$  potential with the concentration of the potential determining ion is also shown graphically in Fig.(5.4).

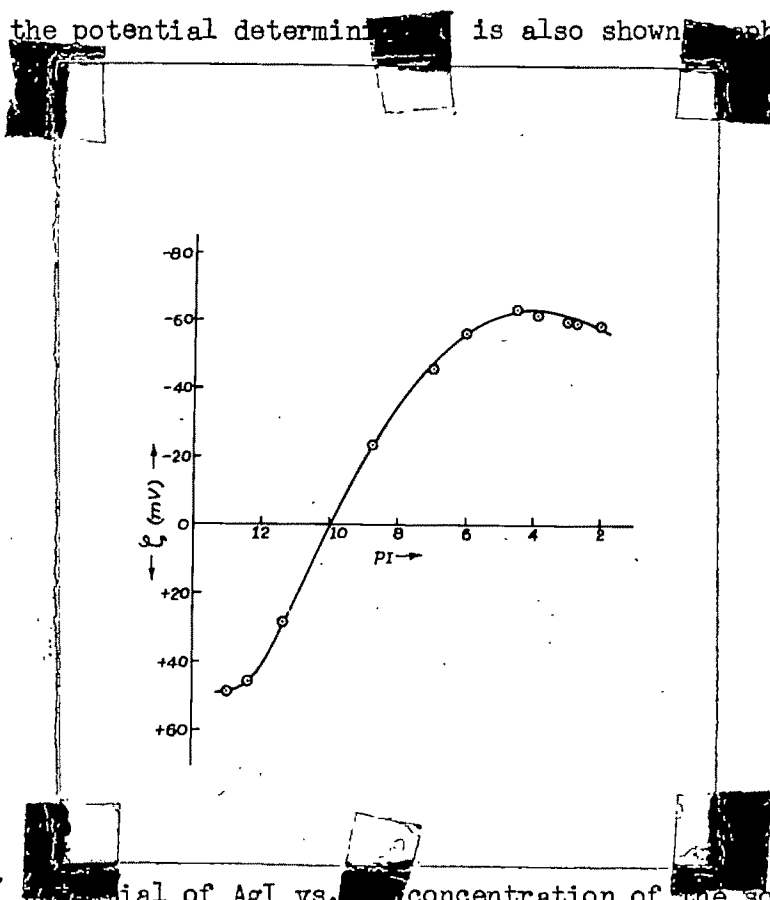


Fig. 5.4.  $\zeta$  potential of AgI vs. concentration of the solution.

(b) For the study of the effect of surface active ions on the mobility (and also  $\zeta$  potential) of AgI particles, at some constant  $I^-$  concentrations (spanning the entire range of variation of  $I^-$  concentration over which the mobility variation of AgI particles has just now been mentioned), the following procedure was followed: Some points on the S-shaped curve (Fig.5.4) corresponding to different  $I^-$  concentrations (four on the negative charge side, and four on the positive charge side) were first selected.\* Different lots of AgI sol with these various  $I^-$  concentrations were

\*Sols with  $I^-$  concentrations too close to the zero point of charge ( $pI^- = 10.0$ ) were found to be unstable and unsuitable for electrophoretic mobility measurements (ref.89).

then prepared in the manner described already, by addition of KI or  $\text{AgNO}_3$  to the stock sol (2nd lot); and their  $\text{I}^-$  concentrations were determined potentiometrically as described.

For each such lot with constant  $\text{I}^-$  concentration the effect of variation of the concentration of surface active counter-ion was then studied (CTA<sup>+</sup> and CPy<sup>+</sup> ions for negatively charged AsI particles and DS<sup>-</sup> for positively charged AsI sol particles). A range of variation of the surfactant concentration from  $\sim 3 \times 10^{-7}$  N to  $\sim 3 \times 10^{-4}$  N was studied. This was below the reported c.m.c. values for these surfactants<sup>98,99</sup>).

The variation of the concentration of surface active ions in the system was effected by adding a very dilute solution of the surfactant of appropriate concentration ( $\sim 10^{-3}$  to  $10^{-5}$  N) to the lot of AgI sol being studied, with a particular constant  $\text{I}^-$  concentration. Starting from the lowest surfactant concentration system, higher concentration systems were obtained by adding the requisite extra amount of surfactant to 150 ml of the solution from the preceding experiment and then making the total volume upto 250 ml again by addition of fresh instalments from the lot of AgI sol being studied. Care was taken to see that the total volume of surfactant solution added was small so as to avoid any appreciable change in the  $\text{I}^-$  concentration of the lot. An interval of  $\sim 2$  hours was allowed each time, so that equilibrium had been attained before any mobility measurement. The constant  $\text{I}^-$  concentration for each lot, as also the different surface active ion concentrations in the system at which mobility measurements were made, are given in Tables (5.2-5.9). The results of mobility measurements together with the values of the other significant parameters are also given in the same Tables (5.2-5.9).

---

\*The c.m.c. values for two of the surfactant samples actually used here (CTAB and CPyCl) were checked by conductivity measurements, and found to agree with the reported values.



3.5. Calculations and results :

The  $\zeta$  potentials were calculated by the W.L.O. method<sup>39</sup>). In the calculation of  $\kappa$ , the concentrations of all the ionic species present in the system were considered where surface active ions were not present ( $\zeta$  vs.  $I^-$  concentration) :

(a) For the system the electrolytes present were KI and  $KNO_3$  on the negative charge side;  $KNO_3$  and  $AgNO_3$  on the positive charge side. (b) In presence of CTAB, for the three systems ( $pI^- = 4.32, 6.68, 7.82$ ) the electrolytes present were KI,  $KNO_3$  and CTAB; and for the system with  $pI^- = 10.77$ , the electrolytes present were  $AgNO_3$ ,  $KNO_3$  and CTAB. (c) Similarly, with (i) NaDS ( $pI^- = 11.11, 11.97$  and  $12.86$ ) and (ii) CPyCl ( $pI^- = 4.47$ ), the electrolytes present in the systems were (i)  $AgNO_3$ ,  $KNO_3$  and NaDS; and (ii) KI,  $KNO_3$  and CPyCl respectively.

Particles of almost same size were chosen for study all-through. Particle size correction was made by using Figs.(3.5 and 3.6). Using for the particle radius ( $a$ ) the value  $0.624 \times 10^{-4}$  cm, the  $\kappa a$  values were calculated.

Since the ions present were not equi-mobile and of ion-conductance different from  $70 \text{ mho.cm}^2$ , therefore the ionic mobility correction had to be introduced in the W.L.O. calculation. The different ion conductance values used<sup>73,98,100</sup> were as follows :

Ions	Ion conductance (mho.cm <sup>2</sup> )	Ions	Ion conductance (mho.cm <sup>2</sup> )
$K^+(23.5^\circ)$	71.44	$NO_3^-(23.5^\circ)$	70.00
$Ag^+(23.5^\circ)$	60.68	$I^-(23.5^\circ)$	74.76
$K^+(30^\circ)$	80.10	$NO_3^-(30^\circ)$	78.80
$Ag^+(30^\circ)$	67.98	$I^-(30^\circ)$	84.05
$CTA^+(30^\circ)$	22.50	$Br^-(30^\circ)$	85.55
$Na^+(30^\circ)$	55.23	$DS^-(30^\circ)$	33.80
$CPy^+(30^\circ)$	24.00	$Cl^-(30^\circ)$	83.52

Since all the systems contained more than one electrolyte, therefore for the calculation of average  $\lambda_{\pm}$  the method of weighted average was used<sup>39</sup>). These average  $\lambda_{\pm}$  values are recorded in the Tables.

CALCULATION OF  $\zeta$  POTENTIAL OF AgI SOL PARTICLES BY THE W.L.O. METHOD

$[KI]$ (N)	$[AgNO_3]$ (M)	$[KNO_3]$ (N)	Sp. cond. (mho/cm)	Time(sec)		Current $\times 10^6$ (amp)	$U \times 10^4$ (cm)	$\lambda$ (av)		m(av)		$E_{\text{expt}}$	Corrected $E'$					$\gamma_0$ (expt)	$\zeta_{\text{W.L.O.}}$ (mV)
				$R_t$	$L_t$			$\lambda_+$	$\lambda_-$	$m_+$	$m_-$		$\gamma_0=1$	2	3	4	5		

Table 5.1 Effect of variation of  $I^-$  concentrations (23.5°C)

Conc. of sol = 0.0361 gm/l;  $d = 2.10 \times 10^{-4}$  cm;  $\alpha = 0.6239 \times 10^{-4}$  cm;  $E'_{\text{expt}} = 0.775 \times 10^4$  x U;  $\zeta_{\text{W.L.O.}} = 25.57 \gamma_0$  (expt) (mV)

$3.36 \times 10^{-5}$		$5.0 \times 10^{-6}$	$7.738 \times 10^{-6}$	9.3	9.2	$61.5 \times 0.2$	-3.595	1.106	71.44	74.13	0.174	0.168	2.786	1.227	2.406	3.153	3.671	3.685	2.48	-63.42
$1.54 \times 10^{-4}$		$5.0 \times 10^{-6}$	$1.80 \times 10^{-5}$	8.5	8.7	27.2	-4.044	1.457	71.44	74.57	0.174	0.167	3.134	1.316	2.515	3.564	4.397	4.689	2.40	-61.37
$1.20 \times 10^{-3}$		$5.0 \times 10^{-6}$	$6.134 \times 10^{-5}$	8.2	8.4	$9.15 \times 10$	-4.277	1.855	71.44	74.73	0.174	0.166	3.330	1.412	2.813	4.059	5.141	5.770	2.35	-60.01
$1.14 \times 10^{-2}$		$5.0 \times 10^{-6}$	$5.018 \times 10^{-4}$	12.6	12.6	49x10	-4.298	2.362	71.44	74.76	0.174	0.166	3.332	1.412	2.88	4.186	5.371	6.233	2.30	-58.80
$2.31 \times 10^{-3}$		$5.0 \times 10^{-6}$	$1.592 \times 10^{-4}$	7.8	7.8	$25.7 \times 10$	-4.398	1.996	71.44	74.74	0.174	0.166	3.409	1.450	2.952	4.302	5.754	6.931	2.32	-59.32
$1.09 \times 10^{-6}$		$3.75 \times 10^{-5}$	$5.914 \times 10^{-6}$	9.0	9.2	$52 \times 0.2$	-3.294	1.101	71.44	70.87	0.174	0.165	2.552	1.226	2.406	3.159	3.629	3.599	2.20	-56.24
$1.33 \times 10^{-7}$		$3.85 \times 10^{-5}$	$6.624 \times 10^{-6}$	9.8	10.0	$59 \times 0.2$	-2.741	1.107	71.44	70.03	0.174	0.177	2.124	1.226	2.405	3.159	3.628	3.599	1.78	-45.51
$1.74 \times 10^{-9}$		$3.86 \times 10^{-5}$	$7.667 \times 10^{-6}$	19.0	19.0	$67 \times 0.2$	-1.592	1.108	71.44	70.02	0.174	0.177	1.122	1.226	2.406	3.159	3.629	3.599	0.90	-23.01
$4.11 \times 10^{-12}$		$3.86 \times 10^{-5}$	$2.269 \times 10^{-5}$	18.8	18.8	35.5	+1.802	1.201	67.64	70.00	0.203	0.178	1.393	1.255	2.422	3.288	3.781	3.777	1.12	+28.64
$4.25 \times 10^{-13}$		$3.86 \times 10^{-5}$	$1.592 \times 10^{-4}$	11.0	11.0	$25.1 \times 10$	+3.050	1.531	62.20	70.00	0.200	0.178	2.363	1.323	2.613	3.500	4.307	4.514	1.78	+45.51
$1.09 \times 10^{-13}$		$3.86 \times 10^{-5}$	$3.85 \times 10^{-4}$	9.4	9.4	66x10	+3.287	1.769	61.20	70.00	0.184	0.178	2.544	1.382	2.720	3.901	4.895	5.440	1.88	+48.07

Table 5.2 Effect of CPyCl at constant  $I^-$  concentration ( $3.36 \times 10^{-5}$  N) (30°C)

Conc. of sol = 0.0361 gm/l;  $[KNO_3] = 5.0 \times 10^{-6}$  N;  $[KI] = 3.36 \times 10^{-5}$  N;  $d = 1.05 \times 10^{-4}$  cm;  $\alpha = 0.6239 \times 10^{-4}$  cm;  $E'_{\text{expt}} = 0.6747 \times 10^4$  x U;  $\zeta_{\text{W.L.O.}} = 26.13 \gamma_0$  (expt) (mV)

$[CPyCl(M)]$	Conc. of sol	$R_t$	$L_t$	Current	$U \times 10^4$	$\log \lambda \alpha$	$\lambda_+$	$\lambda_-$	$m_+$	$m_-$	$E_{\text{expt}}$	Corrected $E'$	$\gamma_0$ (expt)	$\zeta_{\text{W.L.O.}}$ (mV)				
$2.114 \times 10^{-6}$	0.0361	14.0	14.4	17.4	-0.844	1.2690	77.16	83.41	0.1867	0.1708	0.6366	1.296	2.546	3.446	4.025	4.152	0.52	-13.59
$1.881 \times 10^{-6}$	0.0361	9.2	9.2	$72 \times 0.2$	-2.347	1.2681	76.96	83.35	0.1850	0.1700	1.578	1.296	2.546	3.446	4.025	4.152	1.20	-31.36
$5.356 \times 10^{-6}$	0.0361	6.8	6.8	$72 \times 0.2$	+2.170	1.2860	72.86	83.42	0.1954	0.1708	1.459	1.298	2.544	3.54	4.09	4.19	1.10	+28.75
$3.069 \times 10^{-5}$	0.0361	3.4	3.5	$73 \times 0.2$	+4.332	1.3847	54.94	83.49	0.2592	0.1707	2.912	1.34	2.59	3.59	4.24	4.50	2.38	+37.89
$3.859 \times 10^{-4}$	0.0361	4.0	4.0	87.5	+3.680	1.7783	23.09	83.51	0.4896	0.1706	2.474	1.42	2.85	4.07	5.164	5.84	1.90	+62.20
$5.284 \times 10^{-7}$	0.0361	4.0	3.9	$64.5 \times 0.2$	-3.977	1.2601	73.84	83.32	0.1806	0.1710	2.674	1.295	2.541	3.425	4.000	4.124	1.90	-49.66

CALCULATION OF  $\bar{C}$  POTENTIAL OF AgI SOL PARTICLES BY THE W.L.O. METHOD (Contd.)

$\bar{C}$ (M)	Sp. cond. (mho/cm)	Time (sec)		Current $\times 10^6$ (amp)	$U \times 10^4$ (cm)	$\log \alpha$	$\lambda$ (av)		$m(\epsilon)$		$E'_{\text{expt}}$	Corrected $E'$					W.L.O. (mV)
		$R_t$	$L_t$				$\lambda_+$	$\lambda_-$	$m_+$	$m_-$		$\gamma_0=1$	2	3	4	5	

Table 5.3 Effect of CTAB at constant  $I^-$  concentration ( $2.084 \times 10^{-7} N$ ) ( $30^\circ C$ )  
 Conc. of sol =  $0.0361 \text{ gm/l}$ ;  $[KNO_3] = 8.7 \times 10^{-6} N$ ;  $d = 105 \times 10^{-6} \text{ cm}$ ;  $\alpha = 0.6239 \times 10^{-4} \text{ cm}$ ;  $[KI] = 2.084 \times 10^{-7} N$ ;  $E'_{\text{expt}} = 0.6747 \times 10^{-4} \text{ xU}$ ;  $\bar{C}_{\text{W.L.O.}} = 26.13 \gamma_0(\text{expt}) \text{ (mV)}$

$3.046 \times 10^{-7}$	$1.023 \times 10^{-5}$	8.8	9.0	17.0	-1.788	0.7958	77.18	78.45	0.1845	0.1816	1.201	1.12	2.20	2.85	3.20	3.20	1.03	-26.92
$0.978 \times 10^{-6}$	$1.08 \times 10^{-5}$	14.6	14.7	18.0	-1.083	0.9619	74.37	79.56	0.1915	0.1793	0.7281	1.18	2.30	3.00	3.40	3.50	0.62	-16.20
$2.577 \times 10^{-6}$	$1.111 \times 10^{-5}$	17.8	17.8	18.0	+0.9389	0.9944	67.15	80.41	0.2119	0.1771	0.6311	1.198	2.348	3.45	3.45	3.36	0.53	+13.86
$5.526 \times 10^{-6}$	$1.127 \times 10^{-5}$	6.9	7.0	17.5	+2.564	1.0437	58.06	81.45	0.2453	0.1749	1.724	1.223	2.357	3.094	3.50	3.45	1.38	+36.07
$0.995 \times 10^{-5}$	$1.065 \times 10^{-5}$	4.5	4.5	18.5	+3.370	1.1018	49.68	82.37	0.2867	0.1729	2.266	1.265	2.408	3.111	3.50	3.50	1.80	+47.04
$3.248 \times 10^{-5}$	$1.095 \times 10^{-5}$	7.5	7.6	9.5	+4.037	1.2779	34.89	84.14	0.4082	0.1692	2.714	1.268	2.497	3.34	3.81	3.83	2.22	+58.02
$0.990 \times 10^{-4}$	$1.095 \times 10^{-5}$	6.7	6.7	11.0	+3.926	1.4710	27.22	84.94	0.5234	0.1677	2.639	1.338	2.57	3.53	4.17	4.28	2.03	+53.06
$3.113 \times 10^{-4}$	$1.341 \times 10^{-5}$	4.5	4.5	25.5	+3.091	1.7170	24.11	85.47	0.5909	0.1666	2.078	1.392	2.72	3.845	4.727	5.23	1.51	+39.48

Table 5.4 Effect of CTAB at constant  $I^-$  concentration ( $1.509 \times 10^{-8} N$ ) ( $30^\circ C$ )  
 Conc. of sol =  $0.0361 \text{ gm/l}$ ;  $[KNO_3] = 8.84 \times 10^{-6} N$ ;  $[KI] = 1.508 \times 10^{-8} N$ ;  $d = 105 \times 10^{-6} \text{ cm}$ ;  $\alpha = 0.6239 \times 10^{-4} \text{ cm}$ ;  $E'_{\text{expt}} = 0.6747 \times 10^{-4} \text{ xU}$ ;  $\bar{C}_{\text{W.L.O.}} = 26.13 \gamma_0(\text{expt}) \text{ (mV)}$

$3.314 \times 10^{-7}$	$2.508 \times 10^{-6}$	7.5	7.5	39x0.2	-1.136	0.9520	77.96	79.02	0.1827	0.1803	0.7837	1.18	2.26	2.95	3.37	3.28	0.57	-17.51
$2.586 \times 10^{-6}$	$9.258 \times 10^{-6}$	12.0	12.0	60x0.2	+1.595	0.9939	67.05	80.30	0.2124	0.1774	1.072	1.198	2.348	3.05	3.453	3.34	0.88	+23.00
$1.083 \times 10^{-5}$	$1.215 \times 10^{-5}$	5.5	5.0	82x0.2	+3.723	1.1113	47.65	82.54	0.2988	0.1726	2.502	1.255	2.392	3.089	3.532	3.50	2.11	+55.14
$3.301 \times 10^{-5}$	$1.341 \times 10^{-5}$	4.8	4.8	19x1	+3.888	1.2753	34.68	84.88	0.4107	0.1699	2.613	1.269	2.557	3.347	3.847	3.847	2.08	+54.37
$0.993 \times 10^{-4}$	$1.897 \times 10^{-5}$	4.1	4.1	33x1	+3.707	1.4815	27.14	85.02	0.5248	0.1675	2.492	1.338	2.597	3.556	4.17	4.28	1.90	+49.66
$3.247 \times 10^{-4}$	$4.320 \times 10^{-5}$	5.5	5.5	93x1	+2.232	1.7259	24.03	85.35	0.5928	0.1669	1.501	1.40	2.737	3.857	4.75	5.23	1.08	+28.48

Table 5.5 Effect of CTAB at constant  $I^-$  concentration ( $1.687 \times 10^{-11} N$ ) ( $30^\circ C$ )  
 Conc. of sol =  $0.0361 \text{ gm/l}$ ;  $[KNO_3] = 8.75 \times 10^{-6} N$ ;  $[AgNO_3] = 5.01 \times 10^{-6} N$ ;  $d = 105 \times 10^{-6} \text{ cm}$ ;  $\alpha = 0.6239 \times 10^{-4} \text{ cm}$ ;  $E'_{\text{expt}} = 0.6747 \times 10^{-4} \text{ xU}$ ;  $\bar{C}_{\text{W.L.O.}} = 26.13 \gamma_0(\text{expt}) \text{ (mV)}$

$3.314 \times 10^{-7}$	$2.254 \times 10^{-4}$	15.1	15.1	43x10	+0.3177	1.0386	78.94	81.88	0.1804	0.1776	0.617	1.22	2.35	3.09	3.50	3.45	0.50	+13.07
$0.994 \times 10^{-6}$	$2.222 \times 10^{-4}$	19.1	19.2	42x10	+0.6931	1.0488	76.30	82.52	0.1866	0.1726	0.466	1.26	2.40	3.10	3.54	3.50	0.38	+9.931
$3.98 \times 10^{-6}$	$2.268 \times 10^{-4}$	11.2	11.3	42x10	+1.275	1.0889	67.01	83.14	0.2122	0.1716	0.856	1.259	2.398	3.10	3.533	3.49	0.55	+16.89
$0.994 \times 10^{-5}$	$2.201 \times 10^{-4}$	5.2	5.2	42x10	+2.727	1.1517	56.01	83.86	0.2533	0.1701	1.833	1.267	2.394	3.195	3.65	3.58	1.45	+37.89
$3.642 \times 10^{-5}$	$2.222 \times 10^{-4}$	3.7	3.7	42.5x10	+3.336	1.3147	38.30	84.34	0.3718	0.1698	2.511	1.279	2.517	3.397	3.947	3.898	2.02	+52.79
$1.196 \times 10^{-4}$	$2.160 \times 10^{-4}$	3.3	3.3	42x10	+4.122	1.5258	28.44	85.15	0.5007	0.1673	2.771	1.318	2.617	3.747	4.348	4.498	2.1	+54.88

Table 5.6 Effect of CTAB at constant  $I^-$  concentration ( $4.764 \times 10^{-5} N$ ) ( $30^\circ C$ )  
 Conc. of sol =  $0.0361 \text{ gm/l}$ ;  $[KNO_3] = 0.5521 \times 10^{-5} N$ ;  $[KI] = 4.383 \times 10^{-5} N$ ;  $d = 105 \times 10^{-6} \text{ cm}$ ;  $\alpha = 0.6239 \times 10^{-4} \text{ cm}$ ;  $E'_{\text{expt}} = 0.6747 \times 10^{-4} \text{ xU}$ ;  $\bar{C}_{\text{W.L.O.}} = 26.13 \gamma_0(\text{expt}) \text{ (mV)}$

$3.314 \times 10^{-7}$	$6.763 \times 10^{-6}$	3.7	3.7	17.5	-2.764	1.3133	79.69	83.47	0.1787	0.1706	1.857	1.28	2.52	3.40	3.95	3.90	1.45	-48.35
$1.033 \times 10^{-6}$	$1.197 \times 10^{-5}$	5.4	5.5	23.0	-2.525	1.3154	79.02	84.12	0.1803	0.1693	1.697	1.28	2.52	3.40	3.95	3.90	1.31	-44.35
$0.952 \times 10^{-5}$	$1.206 \times 10^{-5}$	6.1	6.3	26.0	+1.977	1.3530	70.84	84.67	0.20	0.1689	1.329	1.294	2.548	3.43	3.946	3.99	1.02	+34.73
$2.561 \times 10^{-5}$	$1.389 \times 10^{-5}$	4.2	4.2	40.0	+2.186	1.4029	60.45	84.77	0.2356	0.1687	1.466	1.297	2.564	3.495	4.10	4.15	1.13	+38.31
$0.923 \times 10^{-4}$	$1.897 \times 10^{-5}$	4.7	4.7	51.5	+2.071	1.5400	42.58	84.84	0.3345	0.1680	1.393	1.32	2.518	3.748	4.348	4.498	1.08	+36.41
$1.88 \times 10^{-4}$	$2.380 \times 10^{-5}$	5.3	5.3	74.0	+1.941	1.6520	34.49	85.17	0.4130	0.1672	1.305	1.378	2.798	3.83	4.70	5.08	1.01	+34.10

[NaDS] (M)	Sp. cond. (mho/cm)	Time (sec)		Current $\times 10^{-6}$ (amp)	$U \times 10^4$ (cm)	log $\kappa a$	$\lambda$ (av)		m (av)	
		$R_t$	$L_t$				$\lambda_+$	$\lambda_-$	$m_+$	$m_-$

Table 5.7 Effect of NaDS at constant  $I^-$  conc  
Conc. of sol = 0.0361 gm/l;  $[KNO_3] = 8.75 \times 10^{-6} N$ ;  $[AgNO_3] = 1.096 \times 10^{-5} N$ ;  $d =$

$2.956 \times 10^{-7}$	1.126	14.0	14.0	34.0	+0.6557	1.1152	73.16	78.15	0.1947	0.1821
$4.121 \times 10^{-6}$	1.40	10.8	10.8	33.5	-1.052	1.1559	67.76	68.03	0.2123	0.2093
$1.027 \times 10^{-5}$	1.48	8.0	8.0	34.0	-1.440	1.1984	64.24	63.30	0.2181	0.2250
$4.165 \times 10^{-5}$	1.83	5.2	5.2	40.0	-2.328	1.3594	61.13	48.41	0.2250	0.2943
$1.03 \times 10^{-4}$	2.431	4.3	4.4	53.0	-2.636	1.5190	58.13	41.05	0.2450	0.3469

Table 5.8 Effect of NaDS at constant  $I^-$  conc  
Conc. of sol = 0.0361 gm/l;  $[KNO_3] = 8.75 \times 10^{-6} N$ ;  $[AgNO_3] = 7.943 \times 10^{-5} N$ ;  $d =$

$2.956 \times 10^{-7}$	4.029	9.6	9.7	83.0	+1.321	1.4378	69.13	78.66	0.2060	0.1811
$0.958 \times 10^{-6}$	3.793	9.6	10.0	83.5	+1.226	1.4386	67.68	78.34	0.2106	0.1818
$3.53 \times 10^{-6}$	3.889	13.0	13.0	81.0	+0.4898	1.4454	64.57	77.07	0.2193	0.1848
$4.142 \times 10^{-5}$	3.950	7.0	7.0	85.0	-1.755	1.5206	61.13	64.37	0.2330	0.2213
$1.194 \times 10^{-4}$	4.773	4.5	4.5	100.0	-2.803	1.6230	57.8	54.09	0.2464	0.2633

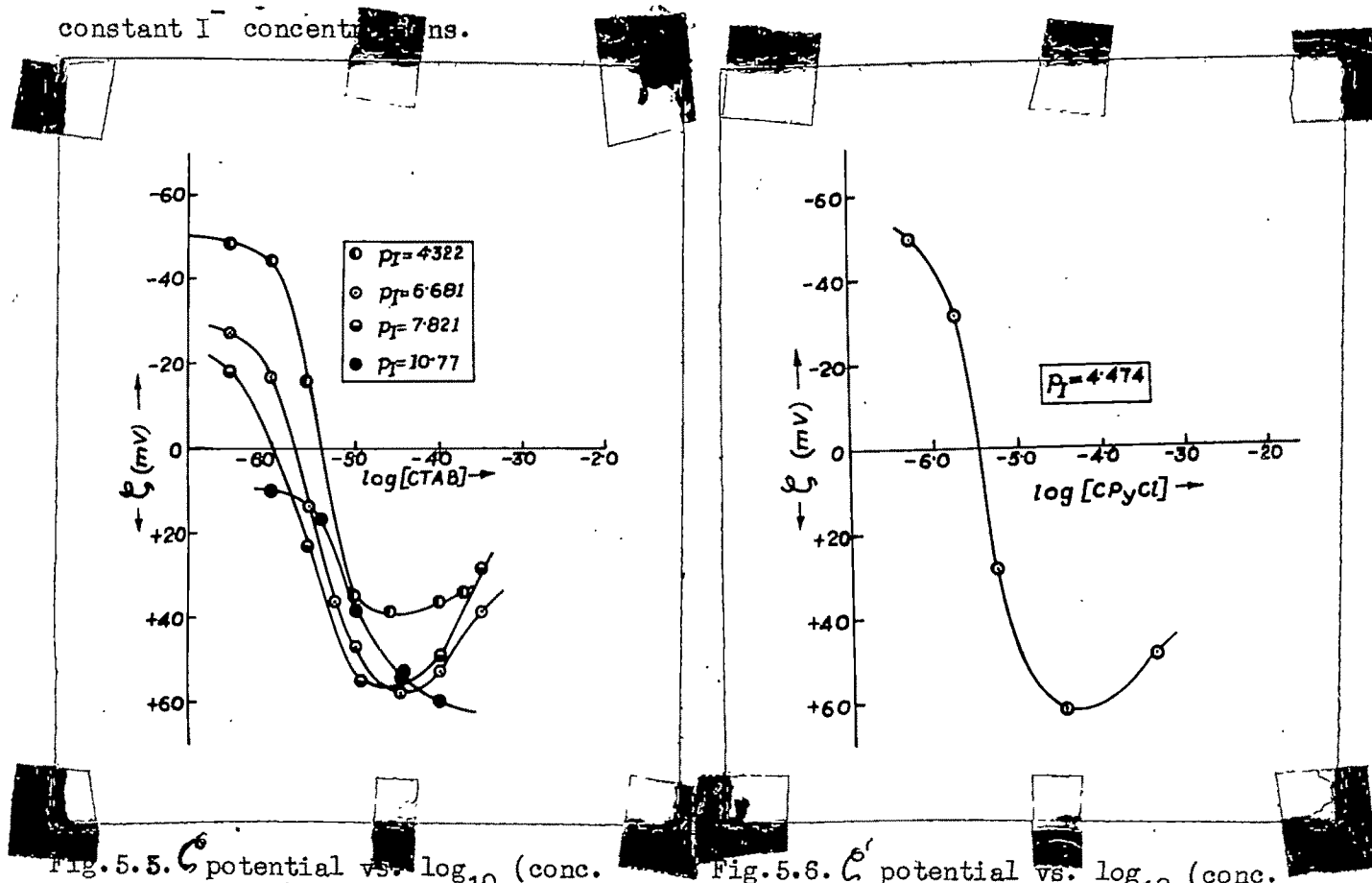
Table 5.9 Effect of NaDS at constant  $I^-$  conc  
Conc. of sol = 0.0361 gm/l;  $[KNO_3] = 8.75 \times 10^{-6} N$ ;  $[AgNO_3] = 6.166 \times 10^{-4} N$ ;  $d = 10$

$2.956 \times 10^{-7}$	3.174	5.5	5.5	62	+2.460	1.8627	68.19	78.77	0.2087	0.1808
$0.958 \times 10^{-6}$	3.111	5.6	5.6	62	+2.369	1.8627	67.68	78.68	0.2091	0.1810
$3.53 \times 10^{-6}$	3.074	6.4	6.4	64.5	+1.968	1.8635	67.02	78.52	0.2102	0.1813
$0.993 \times 10^{-5}$	3.111	9.0	9.0	62	+1.475	1.8657	66.57	78.09	0.2114	0.1824
$5.325 \times 10^{-5}$	3.248	11.0	11.0	62	-1.231	1.8802	66.12	75.26	0.2134	0.1892
$1.502 \times 10^{-4}$	3.241	5.0	5.0	62	-2.828	1.9192	65.64	70.08	0.2170	0.2032

The ionic mobility correction to the particle mobility function  $E'$  was made in the manner indicated earlier, both in the case of positively and negatively charged particles. As the electrolytes were of the 1-1 type, therefore Tables (1.1) and (1.3) respectively (together with equation 1.41) were used for the two cases.

For systems without surfactant ions, the net corrections ( $\Delta E'$ ) were insignificantly small, because the counter-ion conductance factor ( $m_{\pm}$ ) was not greatly different from the reference value 0.184. For the CTAB and CPyCl systems,  $m_{+} > 0.184$  and  $m_{-} < 0.184$ ; so, the said corrections were opposite in sign and counter balanced each other, so that the net correction  $\Delta E'$  was negligible. But for the NaDS system both  $m_{\pm} > 0.184$ , so the  $\Delta E'$  corrections were more or less significant.

The calculated  $\zeta_{W.L.O.}$  values are recorded in Tables (5.1-5.9). The variation of the  $\zeta$  potential of AgI particles with the  $I^{-}$  concentration of the solution is shown in Fig. 5.4, whereas Figs. 5.5, 5.6 and 5.7 show respectively the variation of  $\zeta$  with the concentration of the surfactant ions  $CTA^{+}$ ,  $CPy^{+}$  and  $DS^{-}$  at some different constant  $I^{-}$  concentrations.



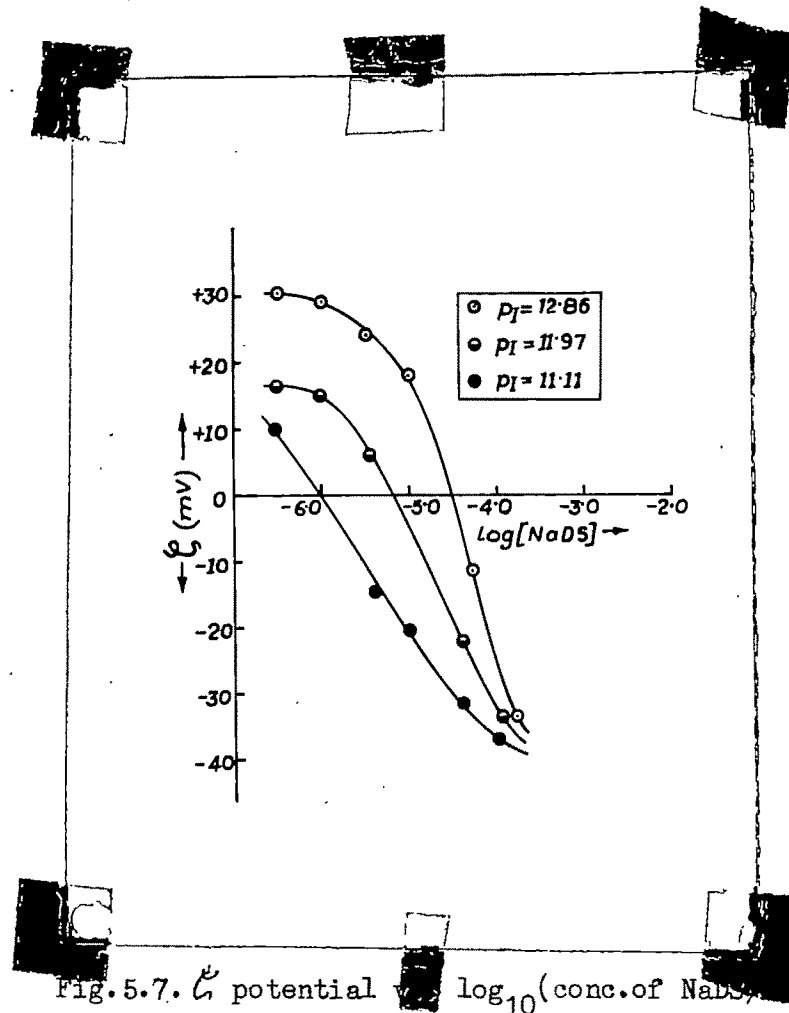


Fig.5.7.  $\zeta$  potential vs  $\log_{10}$ (conc.of NaDS)

5.6. Discussion :

(a) From the variation of the  $\zeta$  potential of AgI sol particles with  $I^-$  ion concentration (Fig.5.4), it is seen that the magnitude of the (negative)  $\zeta$  potential decreases with decreasing  $I^-$  ion concentration; the point of zero charge is reached at  $pI^- = 10$ , and eventually at still lower  $pI^-$  values ( $Ag^+$  excess in solution) the sol becomes gradually more and more positively charged. This behaviour is in full accord with the results reported by earlier workers<sup>101)</sup>; also the mobility at  $pI^- = 4$  is found to be  $3.7 \times 10^{-4}$  cm/sec/V/cm (mobility vs.  $pI^-$  plot not shown), which agrees with that reported by Kruyt and van Gils<sup>102)</sup> ( $3.5 \pm 0.1 \times 10^{-4}$  cm). However, the calculated  $\zeta$  potential shows a maximum value of 64.0 mVs at  $pI^- = 4.0$ , which is lower than the reported maximum value of  $\sim 80.0$  mVs<sup>55)</sup>. Also, the reported<sup>55)</sup> zero point of charge is slightly different (at  $pI^- = 10.6$ ) from that found by us.

(b) The effect of variation of the concentration of surface active counter-ions,

for negatively charged AgI particles at different constant concentrations of  $I^-$  ions, is shown in Fig.5.5 (CTAB) and Fig.5.6 (CPyCl). It is seen that increasing the surface active cation concentration decreases (and eventually reduces to zero) the mobility value for each particular (constant)  $I^-$  ion concentration; at still large concentrations the positive mobility increases further, until (near about the c.m.c.) the mobility becomes more or less constant. Also, the smaller the constant  $I^-$  concentration, the lower is the surfactant counter-ion concentration necessary to reduce the particle mobility to zero. For positively charged AgI particles, the addition of  $CTA^+$  increases the positive mobility right from the beginning; this curve is thus essentially identical with the positive mobility part of the other curves.

In the case of the surfactant CPyCl, electrophoretic mobilities at only a single constant  $I^-$  concentration have been studied. The results are essentially similar to those with CTAB. The two surface active cations used viz.  $CTA^+$  and  $CPy^+$  differ in respect to the head group size. Comparing the  $CPy^+$  curve ( $pI^- = 4.474$ ) with the  $CTA^+$  curve at  $pI^- = 4.372$ , one sees that the surfactant concentration at which the zero point of charge is reached in the two cases are respectively  $3.98 \times 10^{-6} M$  and  $3.76 \times 10^{-6} M$ ; this shift is in the same direction as found by earlier workers<sup>89)</sup> (decrease of head group size shifts to higher values, the zero-charge surfactant concentration).

The effect of negatively charged counter-ion ( $DS^-$ ) on positively charged AgI sol (shown in Fig.5.7) is essentially similar to that in the reverse case discussed above. The positive mobility is more markedly depressed (for the same surfactant concentration), and the charge reversal occurs at lower surfactant concentration, the lower the (constant)  $Ag^+$  ion concentration.

(c) The general shape of the curves corresponds to the theoretical predictions<sup>88)</sup>. The curves have an extended S-shape; also in the region of the zero point of charge, the slopes are more or less identical. In view of the difficulty of mobility measurement near the zero-point of charge more experimental points could not be

secured here, which would be desirable. The theory predicts that all curves should have the same slope at the region of the zero point of charge<sup>89)</sup>. In the following table the concentration of surface active agent at the zero point of charge, as also the slopes of the curves at this point are recorded.

Table 5.10. Concentration of surface-active counter-ion and  $(d\zeta/d \log M)_{\zeta=0}$  at zero point of charge.

Surface-active ion	pI <sup>-</sup>	Surfactant concentration (M)	$(d\zeta/d \log M)_{\zeta=0}$
CTA <sup>+</sup>	4.322	$3.758 \times 10^{-6}$	94.3
	6.681	$1.778 \times 10^{-6}$	56.7
	7.821	$9.441 \times 10^{-7}$	36.7
	10.770	-	-
CPy <sup>+</sup>	4.474	$3.981 \times 10^{-6}$	103.3
DS <sup>-</sup>	11.11	$1.259 \times 10^{-6}$	40.0
	11.97	$6.761 \times 10^{-6}$	22.9
	12.86	$2.818 \times 10^{-5}$	18.0